True Gravity in Atmospheric Ekman Layer Dynamics

Peter C Chu[1]

[1]Naval Postgraduate School

November 26, 2022

Abstract

True gravity is a three-dimensional vector, g = igλ+jgφ+kgz, with (λ, φ, z) the (longitude, latitude, height) and (i, j, k) the corresponding unit vectors. The vertical direction is along g, not along k, which is normal to the Earth spherical (or ellipsoidal) surface (called deflected-vertical). Correspondingly, the spherical (or ellipsoidal) surfaces are not horizontal surfaces (called deflected-horizontal surfaces). In the (λ, φ, z) coordinates, the true gravity g has longitudinal-latitudinal component, gh = igλ+jgφ, but it is neglected completely in meteorology through using the standard gravity (-g0k, g0 = 9.81 m/s2) instead. Such simplification on the true gravity g has never been challenged. This study uses the atmospheric Ekman layer as an example to illustrate the importance of gh. The standard gravity (-g0k) is replaced by the true gravity g in the classical atmospheric Ekman layer equation with a constant eddy viscosity (K) and a height-dependent-only density ρ(z) represented by an e-folding stratification. New formulas for the Ekman spiral and Ekman pumping are obtained. The second derivative of the gravity disturbance (T) versus z, also causes the Ekman pumping, , in addition to the geostrophic vorticity with DE the Ekman layer thickness and f the Coriolis parameter. With data from the EIGEN-6C4 static gravity model, the global mean strength of the Ekman pumping due to the true gravity is found to be 4.0 cm s-1. Such evidently large value implies the urgency to include the true gravity g into the atmospheric dynamics.

True Gravity in Atmospheric Ekman Layer Dynamics

Peter C. Chu

Department of Oceanography, Naval Postgraduate School, Monterey, CA, USA.

Corresponding author: Peter Chu (pcchu@nps.edu)

Key Points:

- Vertical that meteorologists think is not vertical. True gravity $\mathbf{g}(\lambda, \varphi, z)$ represents vertical with latitudinal-longitudinal components
- Replacement of the standard gravity $-g_0\mathbf{k}$ (g_0=9.81 m s^{-2}) by $\mathbf{g}(\lambda, \varphi, z)$ in the classical Ekman layer equation leads to a new solution
- With data from the EIGEN-6C4 static gravity model, the global mean strength of the Ekman pumping due to $\mathbf{g}(\lambda, \varphi, z)$ is 4.0 cm s^{-1}.

Abstract

True gravity is a three-dimensional vector, $\mathbf{g} = \mathbf{i}g_\lambda+\mathbf{j}g_\varphi+\mathbf{k}g_z$, with ($\lambda$, φ, z) the (longitude, latitude, height) and (**i**, **j**, **k**) the corresponding unit vectors. The vertical direction is along **g**, not along **k**, which is normal to the Earth spherical (or ellipsoidal) surface (called deflected-vertical). Correspondingly, the spherical (or ellipsoidal) surfaces are not horizontal surfaces (called deflected-horizontal surfaces). In the (λ, φ, z) coordinates, the true gravity **g** has longitudinal-latitudinal component, $\mathbf{g}_h = \mathbf{i}g_\lambda+\mathbf{j}g_\varphi$, but it is neglected completely in meteorology through using the standard gravity ($-g_0\mathbf{k}$, g_0 = 9.81 m/s^2) instead. Such simplification on the true gravity **g** has never been challenged. This study uses the atmospheric Ekman layer as an example to illustrate the importance of $\mathbf{g}_h$. The standard gravity ($-g_0\mathbf{k}$) is replaced by the true gravity **g** in the classical atmospheric Ekman layer equation with a constant eddy viscosity (K) and a height-dependent-only density $\rho(z)$ represented by an e-folding stratification. New formulas for the Ekman spiral and Ekman pumping are obtained. The second derivative of the gravity disturbance (T) versus z, also causes the Ekman pumping, $(D_E / 2\pi f)\partial^2 T / \partial z^2$, in addition to the geostrophic vorticity with D_E the Ekman layer thickness and f the Coriolis parameter. With $\partial^2 T / \partial z^2$ data from the EIGEN-6C4 static gravity model, the global mean strength of the Ekman pumping due to the true gravity is found to be 4.0 cm s^{-1}. Such evidently large value implies the urgency to include the true gravity **g** into the atmospheric dynamics.

Plain Language Summary

Meteorologists use the spherical (or ellipsoidal) surfaces represented by latitude (φ) and longitude (λ) as the horizontal and the direction normal to them represented by height (z) as the vertical. It is not correct since the vertical direction is represented by the true gravity $\mathbf{g}(\lambda, \varphi, z)$; and the horizontal surfaces are the equipotential surfaces of $\mathbf{g}(\lambda, \varphi, z)$ such as the geoid surface which is nearest to the Earth spherical (or ellipsoidal) surface (z = 0). In the (λ, φ, z) coordinates, the true gravity $\mathbf{g}(\lambda, \varphi, z)$ has latitudinal and longitudinal components, which are neglected completely in meteorology. This study uses the atmospheric Ekman layer dynamics and the true gravity data from the EIGEN-6C4 static gravity model as an example to show the importance of using the true gravity $\mathbf{g}(\lambda, \varphi, z)$ in the atmospheric dynamics.

1 Introduction

Meteorologists usually use the Earth-fixed coordinate system with (λ, φ, z) representing the longitude, latitude, and spherical normal (or height) with (**i**, **j**, **k**) the corresponding unit vectors. The unit vector **k** does not represent the vertical direction since the Earth true gravity **g** ($= g_\lambda\mathbf{i} + g_\varphi\mathbf{j} + g_z\mathbf{k}$) represents the vertical. We may call the direction of **k** the deflected-vertical. The angle between **-k** and **g** is the vertical deflection. The spherical (or ellipsoidal) surfaces are not the horizontal surfaces since the equipotential surfaces of **g** such as the geoid surface represent the horizontal surfaces. We may call the spherical (or ellipsoidal) surfaces the deflected-horizontal surfaces. Appendix A provides difference between the oblate spheroid (ellipsoidal) coordinates versus polar spherical coordinates.

The turbulent mixing in atmospheric planetary boundary layer is treated as a diffusion process similar to molecular diffusion, with an eddy viscosity K, which is many orders of magnitude larger than the molecular viscosity. The turbulent mixing generates ageostrophic wind (called the Ekman spiral), decaying by an e-folding over a height as the wind vector rotate to the right (left) in the northern (southern) hemisphere through one radian (Ekman, 1905). Along with the Ekman spiral, several important processes such as Ekman pumping can be identified.

As in other atmospheric dynamics, the Ekman theory was established using the standard gravity ($-g_0\mathbf{k}$, g_0 = 9.81 m s^{-2}), rather than the true gravity $\mathbf{g}$ (Pedlosky, 1987; Holton, 2004). Its longitudinal-latitudinal component, $\mathbf{g}_h$ ($= g_\lambda\mathbf{i} + g_\varphi\mathbf{j}$), is neglected completely. Use of the standard gravity ($-g_0\mathbf{k}$) instead of the true gravity $\mathbf{g}$ is based on the comparison that the strength of the deflected-vertical component $|g_z|$ is 5-6 orders of magnitude larger than the strength of the deflected-horizontal gravity $|\mathbf{g}_h|$. This comparison is unphysical because such a huge difference in magnitude between the components in $\mathbf{k}$ and in ($\mathbf{i}$, $\mathbf{j}$) also occurs in the pressure gradient force in large-scale atmospheric dynamics. But, the pressure gradient force in ($\mathbf{i}$, $\mathbf{j}$) is never neglected against the pressure gradient force in $\mathbf{k}$. Thus, the feasibility of using the standard gravity ($-g_0\mathbf{k}$) in meteorology needs to be investigated. The Ekman dynamics provides a theoretical framework for such a study.

The rest of the paper is outlined as follows. Section 2 presents the dynamic equation with the true gravity for atmospheric Ekman layer. Section 3 shows the Ekman layer solution and a new equation for the Ekman pumping due to the use of the true gravity. Section 4 describes the data source (EIGEN-6C4 model) of the second derivative of the disturbing static gravity potential ($\partial^2 T/\partial z^2$), and shows the Global Ekman pumping velocity due to $\partial^2 T/\partial z^2$ using the EIGEN-6C4 data. Section 5 shows the feasibility of using the (λ, φ, z) coordinates. Section 6 presents the conclusions. Appendices A-D present the two Earth coordinate systems and the basic information about the true gravity $\mathbf{g}$ and related disturbing static gravity potential T.

2 Dynamic Equation with the True Gravity

Steady-state large-scale atmospheric dynamic equation with the Boussinesq approximation (replacement of density ρ by a constant ρ_0 except ρ being multiplied by the gravity and incompressibility) is given by (Chu, 2021)

$$\rho_0\left[2\boldsymbol{\Omega}\times\mathbf{U}\right] = -\nabla_3 p + \rho\mathbf{g} + \rho_0\mathbf{F} \tag{1a}$$

$$\nabla \bullet \mathbf{U} + \frac{\partial w}{\partial z} = 0 \tag{1b}$$

if the pressure gradient force, true gravity $\mathbf{g}$ (see Appendices B and C), and friction are the only real forces. Here, $\nabla_3 \equiv \mathbf{i}\frac{1}{R\cos\varphi}\frac{\partial}{\partial\lambda} + \mathbf{j}\frac{1}{R}\frac{\partial}{\partial\varphi} + \mathbf{k}\frac{\partial}{\partial z}$, and $\nabla \equiv \mathbf{i}\frac{1}{R\cos\varphi}\frac{\partial}{\partial\lambda} + \mathbf{j}\frac{1}{R}\frac{\partial}{\partial\varphi}$ are the 3D and 2D vector differential operators in the polar spherical coordinates; $\boldsymbol{\Omega} = \Omega\left(\mathbf{j}\cos\varphi + \mathbf{k}\sin\varphi\right)$, is the Earth rotation vector with $\Omega = 2\pi/(86164\ \text{s})$ the Earth rotation rate; ρ is the density; ρ_0 = 1.225 kg/m^3, is the characteristic density near the ocean surface; $\mathbf{U} = (u, v)$, is the deflacted-horizontal velocity vector; w is the deflacted-vertical velocity; p is the pressure; and $\mathbf{F}$ is the turbulent diffusive force due to the vertical shear represented by

$$\mathbf{F} = \frac{\partial}{\partial z}\left(K\frac{\partial\mathbf{U}}{\partial z}\right) \tag{2}$$

Let $\mathbf{U}_g$ be the geostrophic wind

$$\rho_0\left[2\boldsymbol{\Omega}\times\mathbf{U}_g\right] = -\nabla p \tag{3}$$

After substitution of (3) into (1a), we get the dynamic equation for the Ekman layer

$$\rho_0\left[2\boldsymbol{\Omega}\times(\mathbf{U}-\mathbf{U}_g)\right] = \rho\mathbf{g}_h + \rho_0\mathbf{F}, \quad \mathbf{g}_h = \mathbf{i}g_\lambda + \mathbf{j}g_\varphi \tag{4}$$

where $\mathbf{g}_h$ is independent on z in the troposphere (see Appendix D).

Baroclinicity (i.e., non-zero latitudinal or longitudinal density gradient) and spatially varying eddy viscosity K affect the Ekman layer dynamics (Chu, 2018; Sun & Sun, 2020). To limit the study on the effect of $\mathbf{g}_h$, the eddy viscosity K is assumed constant and the density varies in the z-direction, i.e., the geostrophic wind does not depend on z,

$$\partial \mathbf{U}_g / \partial z = 0 .$$

Furthermore, a special density stratification is selected for this study as the e-folding decreasing with height

$$\frac{\rho}{\rho_0} = s(z), \quad s(z) \equiv \exp\left(-\frac{z}{H}\right), \qquad H = 10.4 \text{ km} \tag{5}$$

where H is considered as the height of the troposphere. Substitution of (5) into (4) leads to

$$2\mathbf{\Omega} \times (\mathbf{U} - \mathbf{U}_g) = s(z)\mathbf{g}_h + K\frac{\partial^2 \mathbf{U}}{\partial z^2} \tag{6}$$

With the complex variables, the deflected-horizontal gravity ($\mathbf{g}_h$), Ekman velocity ($\mathbf{U}$), and geostrophic wind ($\mathbf{U}_g$) are defined by

$$G_h = g_\lambda + i g_\varphi, \; U = u_E + i v_E, \; U_g = u_g + i v_g, \; i \equiv \sqrt{-1} \tag{7}$$

Eq.(6) is converted into

$$\frac{\partial^2 U}{\partial z^2} - i\frac{f}{K}(U - U_g) = -\frac{s(z)}{K} G_h . \tag{8}$$

Substitution of (5) into (8) leads to

$$\frac{\partial^2 U}{\partial z^2} - i\frac{f}{K}(U - U_g) = -\frac{G_h}{K}\exp\left(-\frac{z}{H}\right) \tag{9}$$

The Ekman velocity U needs to be satisfied by the upper boundary condition,

$$U \to U_g \;\; \text{as} \;\; z \to \infty \tag{10}$$

and the surface`s boundary condition

$$U = 0 \;\; \text{as} \;\; z = 0 \tag{11}$$

3 Ekman Layer Solution

Eq.(9) with the boundary conditions (10) and (11) has the exact solution

$$U(z) = U_g - \left[U_g - \Gamma(\delta^2 + 2i)G_h\right]e^{-(1+i)\pi z/D_E} - \Gamma(\delta^2 + 2i)G_h e^{-z/H} \tag{12}$$

where

$$D_E \equiv \pi\sqrt{\frac{2K}{|f|}}, \quad \delta \equiv \frac{D_E}{\pi H} = \frac{\sqrt{2K/|f|}}{H}, \;\; \Gamma \equiv \frac{2}{f(\delta^4 + 4)} \tag{13}$$

Here, D_E is the Ekman layer depth; and δ is the ratio between the Ekman layer depth (D_E) and the height of troposphere (H). Converting the Ekman layer spiral (12) into the vector form

$$u = u_g - \left\{ \left[u_g - \Gamma(\delta^2 g_\lambda - 2g_\varphi) \right] \cos\left(\frac{\pi z}{D_E} \right) + \left[v_g - \Gamma(\delta^2 g_\varphi + 2g_\lambda) \right] \sin\left(\frac{\pi z}{D_E} \right) \right\} e^{-\pi z / D_E}$$
$$- \Gamma(\delta^2 g_\lambda - 2g_\varphi) e^{-z/H}$$
$$v = v_g - \left\{ -\left[u_g - \Gamma(\delta^2 g_\lambda - 2g_\varphi) \right] \sin\left(\frac{\pi z}{D_E} \right) + \left[v_g - \Gamma(\delta^2 g_\varphi + 2g_\lambda) \right] \cos\left(\frac{\pi z}{D_E} \right) \right\} e^{-\pi z / D_E}$$
$$- \Gamma(\delta^2 g_\varphi + 2g_\lambda) e^{-z/H} \tag{14}$$

The eddy viscosity K is taken as a constant (K = 5 m^2 s^{-1}) in the atmospheric planetary boundary layer (Holton, 2004). The parameter δ is estimated by

$$\delta = \frac{\sqrt{2K/|f|}}{H} = \frac{0.0252}{\sqrt{|\sin\varphi|}}, \quad \text{for } K = 5 \text{ m}^2\text{s}^{-1},\ H = 10.4 \text{ km},\ \Omega = \frac{2\pi}{86164 \text{ s}} \tag{15}$$

where the parameter δ varies from 0.0854 at φ=5º (*N* or *S*) to 0.0252 at φ=90º (*N* or *S*). The range of $\pi\delta$ and the maximum values of δ^2 (at *φ*=5º S or N) are estimated by

$$0.07917 \le \pi\delta \le 0.2683, \quad \delta^2 \le 0.7286 \times 10^{-2} \tag{16}$$

It is reasonable to delete terms with δ^2 in (14). The Ekman profile (14) is simplified by

$$u = u_g - \left[\left(u_g + \frac{g_\varphi}{f} \right) \cos\left(\frac{\pi z}{D_E} \right) + \left(v_g - \frac{g_\lambda}{f} \right) \sin\left(\frac{\pi z}{D_E} \right) \right] e^{-\pi z/D_E} + \frac{g_\varphi}{f} e^{-z/H}$$
$$v = v_g - \left[-\left(u_g + \frac{g_\varphi}{f} \right) \sin\left(\frac{\pi z}{D_E} \right) + \left(v_g - \frac{g_\lambda}{f} \right) \cos\left(\frac{\pi z}{D_E} \right) \right] e^{-\pi z/D_E} - \frac{g_\lambda}{f} e^{-z/H} \tag{17}$$

where the parameter Γ is simplified as $\Gamma = 1/(2f)$. Substitution of (17) into the continuity equation (1b) and integration with respect to *z* from *z* = 0 to *z* = D_E leads to

$$w(D_E) = \frac{1}{R} \int_0^{D_E} \left(\frac{1}{\cos\varphi} \frac{\partial u}{\partial \lambda} + \frac{\partial v}{\partial \varphi} \right) dz \tag{18}$$

Substitution of (17) into (18) gives the Ekman pumping velocity

$$w(D_E) = \frac{D_E}{2\pi} \zeta_g - \frac{D_E}{2\pi f} \nabla \bullet \mathbf{g}_h \tag{19}$$

where the following approximations in the definite integration (18) are used

$$e^{-\pi} = 0.04321 \ll 1, \quad e^{-\pi\delta} \approx 1 \tag{20}$$

Here, $\zeta_g = \mathbf{k} \bullet \nabla \times \mathbf{U}_g$ is the geostrophic vorticity. Eq.(19) clearly shows that $\nabla \bullet \mathbf{g}_h$ causes the Ekman pumping in addition to the geostrophic vorticity. Substitution of (D6) in Appendix D into (19) leads to

$$\boxed{w(D_E) = \frac{D_E}{2\pi} \zeta_g + \frac{D_E}{2\pi f} \frac{\partial^2 T}{\partial z^2} \Big|_{z=0}} \tag{21}$$

where *T* is the disturbing static gravity potential (see Appendices C and D). The second term in the righthand side of (21) is the Ekman pumping due to the use of the true gravity

$$\boxed{w_{tg}(D_E) = \frac{D_E}{2\pi f} \frac{\partial^2 T}{\partial z^2} \Big|_{z=0}} \tag{22}$$

Here, the second derivative of the disturbing static gravity potential ($\partial^2 T/\partial z^2$) is obtained from a gravity model from the geodetic community.

4 Global Ekman Pumping Velocity Due to $\partial^2 T/\partial z^2$

The global data of the second derivative of the disturbing static gravity potential $\partial^2 T/\partial z^2$ is obtained from the global static gravity model EIGEN-6C4 (http://icgem.gfz-potsdam.de/home) (Kostelecký et al. 2015), which was developed jointly by the GFZ Potsdam and GRGS Toulouse up to degree and order 2190, on 1°×1° grids (Figure 1), with -603.6 Eotvos as the minimum and 642.8 Eotvos as the maximum (1 Eotvos = 10^{-9} s^{-2}). With the openly available data of $\partial^2 T/\partial z^2$, the Ekman pumping velocity due the use of the true gravity is easily identified. The global Ekman pumping velocity due to the true gravity $w_{tg}(D_E)$ (Figure 2) is calculated using (22) with the EIGEN-6C4 $\partial^2 T/\partial z^2$ data. The equatorial region (5°S – 5°N) is not included since the geostrophic balance does not exist there. Histogram of $w_{tg}(D_E)$ shows the Gaussian type distribution (Figure 3a), and histogram of $|w_{tg}(D_E)|$ shows the near Gamma distribution with the mean of 4.0 cm s^{-1}, and standard deviation of 13.59 cm s^{-1}. The result that the global mean $|w_{tg}(D_E)|$ reaches an evidently large value of 4.0 cm s^{-1} indicates the importance of $\partial^2 T/\partial z^2$ in atmospheric Ekman pumping.

5 True-Vertical Coordinate versus Deflected-Vertical Coordinate

As mentioned in the Introduction section, the true vertical direction $\mathbf{e}_3$ (upward positive) is with the true gravity **g**,

$$\mathbf{g}(\lambda,\varphi,z) = -\left|\mathbf{g}(\lambda,\varphi,z)\right|\mathbf{e}_3(\lambda,\varphi,z)\,. \tag{23}$$

The true horizonal surfaces are the equipotential surfaces of the true gravity $[V(\lambda,\varphi,z)]$ (see Appendix C). The geoid is one of them. On a true horizontal surface, the orthogonal unit vectors are represented by $[\mathbf{e}_1(\lambda,\varphi,z),\ \mathbf{e}_2(\lambda,\varphi,z)]$, but not (**i**, **j**). With such a true-vertical coordinate, the true gravity **g** has the vertical component only with no true-horizontal component. This treatment seems attractive to meteorologist. However, it is not feasible at all since the unit vectors $[\mathbf{e}_1(\lambda,\varphi,z),\ \mathbf{e}_2(\lambda,\varphi,z),\mathbf{e}_3(\lambda,\varphi,z)]$ vary at each point inside the troposphere, and it is almost impossible to convert any atmospheric model (theoretical or numerical) with the standard gravity ($-g_0\mathbf{k}$) into the model with the true gravity **g** using the reference coordinates with the unit vectors $[\mathbf{e}_1(\lambda,\varphi,z),\ \mathbf{e}_2(\lambda,\varphi,z),\mathbf{e}_3(\lambda,\varphi,z)]$. The alternative treatment is to keep the deflected-vertical direction **k** and deflected-horizontal surface (**i**, **j**) as the same as the meteorologists use. With this treatment, the unit vectors (**i**, **j**, **k**) are independent on (λ, φ, z). It is easy to replace the standard gravity ($-g_0\mathbf{k}$) by the true gravity $\mathbf{g}$ (= $\mathbf{g}_h - g_0\mathbf{k}$) into any atmospheric models.

6 Conclusions

Meteorologists use the deflected-vertical (i.e., normal to the Earth spherical/ellipsoidal surface) as the "vertical", the deflacted-horizontal (i.e., the Earth spherical/ellipsoidal surfaces) as the "horizontal", and the standard gravity ($-g_0$)**k** instead of the true gravity **g**. The true gravity **g** has latitudinal-longitudinal (i.e., deflected-horizontal) component $\mathbf{g}_h$, which is neglected completely. This study demonstrates the importance of $\mathbf{g}_h$ in atmospheric dynamics using the Ekman layer as an example. With the constant eddy viscosity *K* and the e-folding type height-decreasing density, new equation for the atmospheric Ekman layer dynamics was derived including both geostrophic forcing and $\mathbf{g}_h$. The evident Ekman pumping velocity due to the true gravity $[w_{tg}(D_E)]$ is identified using the openly available data of $\partial^2 T / \partial z^2$ (T is the disturbing static gravity potential) from the EIGEN-6C4 gravity model with the global mean of 4.0 cm s^{-1} (evidently large) and standard deviation of 13.59 cm s^{-1} for $|w_{tg}(D_E)|$. Note that the results in this study is only for the specially selected density field represented by the e-folding density stratification with one specific gravity model (i.e., EIGEN-6C4), not for the density in the real atmosphere. However, it demonstrates that $\mathbf{g}_h$ is an important forcing term in the atmospheric dynamics. Finally, if the meteorological community wants to keep the traditional terminology about the vertical (normal to the Earth sphere/ellipsoid) and horizontal (Earth spherical/ellipsoidal surface), the direction along the true gravity vector $\mathbf{g}$ ($= \mathbf{i}g_\lambda + \mathbf{j}g_\varphi + \mathbf{k}g_z$) should be called the ***true vertical***; and the equipotential surfaces such as the geoid should be called the ***true horizontal***.

Appendix A. Oblate Spheroid Coordinates Versus Polar Spherical Coordinates

The oblate spheroid coordinates share the same longitude (λ) but different latitude (φ_{ob}) and radial coordinate (representing vertical) (r_{ob}) with corresponding unit vectors (**i**, **j**, **k**). The relationship between the oblate spheroid coordinates (λ, φ_{ob}, r_{ob}) and the polar spherical coordinates (λ, φ, r) is given by (Gill, 1982)

$$r^2 = r_{ob}^2 + \frac{1}{2}d^2 - d^2 \sin^2 \varphi_{ob}, \quad r^2 \cos^2 \varphi = (r_{ob}^2 + \frac{1}{2}d^2)\cos^2 \varphi_{ob} \qquad \text{(A1)}$$

where d is the half distance between the two foci of the ellipsoid. For the normal Earth, $d = 521.854$ km. The 3D vector differential operator in the oblate spheroid coordinates is represented by

$$\nabla_3 = \mathbf{i}\frac{1}{h_\lambda^{ob}}\frac{\partial}{\partial \lambda} + \mathbf{j}\frac{1}{h_\varphi^{ob}}\frac{\partial}{\partial \varphi} + \mathbf{k}\frac{1}{h_r^{ob}}\frac{\partial}{\partial z}, \qquad z = r - R \qquad \text{(A2)}$$

where $R = 6.3781364\times10^6$ m, is the semi-major axis of the normal Earth (Earth radius). The coefficients (or called Lame numbers) (h_λ^{ob}, h_φ^{ob}, h_r^{ob}) are given by

$$h_\lambda^{ob} = \sqrt{r^2 + \frac{1}{2}d^2}\cos\varphi, \quad h_\varphi^{ob} = \sqrt{r^2 - \frac{1}{2}d^2 + d^2\sin^2\varphi}, \quad h_r^{ob} = \frac{r\sqrt{r^2 - \frac{1}{2}d^2 + d^2\sin^2\varphi}}{\sqrt{r^4 - \frac{1}{4}d^4}}. \qquad \text{(A3)}$$

However, the 3D vector differential operator in the polar spherical coordinates is represented by

$$\nabla_3 = \mathbf{i}\frac{1}{R\cos\varphi}\frac{\partial}{\partial\lambda} + \mathbf{j}\frac{1}{R}\frac{\partial}{\partial\varphi} + \mathbf{k}\frac{\partial}{\partial z}. \qquad \text{(A4)}$$

The difference between the two coordinates is 0.17% (Gill, 1982).

Appendix B. True Gravity and Its approximation

The true gravity **g** is represented by a three-dimensional vector in the (λ, φ, z) coordinate system,

$$\mathbf{g} = \mathbf{g}_h + \mathbf{k}g_z, \quad \mathbf{g}_h = \mathbf{i}g_\lambda + \mathbf{j}g_\varphi \qquad \text{(B1)}$$

where $\mathbf{g}_h$ is its deflected-horizontal component, and $g_z\mathbf{k}$ the deflected-vertical component. It has two approximated forms. The first one is the normal gravity $[-g(\varphi)\mathbf{k}]$ and usually represented in the oblate spheroid coordinates (see Appendix A) and associated with a mathematically modeled

Earth (i.e., a rigid and geocentric ellipsoid) called the normal Earth. The normal Earth is a spheroid (i.e., an ellipsoid of revolution), has the same total mass and angular velocity as the Earth, and coincides its minor axis with the mean rotation of the Earth (Vaniček & Krakiwsky, 1986). The normal gravity vector [$-g(\varphi)\mathbf{k}$] is the sum of the gravitational and centrifugal accelerations exerted on the water particle by the normal Earth. Its intensity $g(\varphi)$ is determined analytically. For example, the World Geodetic System 1984 uses the Somiglina equation (National Geospatial-Intelligence Agency, 1984) to represent $g(\varphi)$

$$g(\varphi) = g_e\left[\frac{1+\kappa\sin^2\varphi}{\sqrt{1-e^2\sin^2\varphi}}\right],\ e^2 = \frac{a^2-b^2}{a^2},\ \kappa = \frac{bg_p - ag_e}{ag_e} \tag{B2}$$

where (a, b) are the equatorial and polar semi-axes; a is used for the Earth radius, $R = a = 6.3781364\times10^6$ m; $b = 6.3567523\times10^6$ m; e is the spheroid's eccentricity; $g_e = 9.780$ m/s^2, is the gravity at the equator; and $g_p = 9.832$ m/s^2 is the gravity at the poles. The second one is the standard gravity vector, $-g_0\mathbf{k}$, with $g_0 = 9.81$ m/s^2. Meteorologist uses the standard gravity. Both normal and standard gravities don't have latitudinal and longitudinal components.

Appendix C. True, Normal, and Standard Gravity Potentials

Let (V, E, E_0) be the gravity potentials associated with the true gravity $\mathbf{g}$, the normal gravity $-g(\varphi)\mathbf{k}$, and the standard gravity $-g_0\mathbf{k}$. The potentials of the normal and standard gravities are given by

$$E(\varphi, z) = -g(\varphi)z, \quad E_0(z) = -g_0 z \tag{C1}$$

Both V and E include the potential of the Earth's rotation (P_R)

$$P_R = \Omega^2 r^2 \cos^2\varphi / 2\ ). \tag{C2}$$

The gravity disturbance is the difference between the true gravity $\boldsymbol{g}(\lambda, \varphi, z)$ and the normal gravity [$-g(\varphi)\mathbf{k}$] at the same point (Hackney & Featherstone 2003). The potential of the gravity disturbance (called the disturbing gravity potential) is given by

$$T = V - E = V + g(\varphi)z \tag{C3}$$

With the disturbing gravity potential T, the true gravity $\mathbf{g}$ (= $\mathbf{g}_h + g_z\mathbf{k}$) and its components are represented by (Sandwell & Smith 1997)

$$\mathbf{g} = \nabla_3 V,\ \ \mathbf{g}_h = \nabla T,\ \ g_z = -g(\varphi) + \frac{\partial T}{\partial z} \tag{C4}$$

where $\nabla \equiv \mathbf{i}\frac{1}{R\cos\varphi}\frac{\partial}{\partial\lambda} + \mathbf{j}\frac{1}{R}\frac{\partial}{\partial\varphi}$ is the 2D vector differential operator. The disturbing static gravity potential (T) outside the Earth masses in the spherical coordinates with the spherical expansion is given by (Kostelecký et al. 2015)

$$T(r,\lambda,\varphi) = \frac{GM}{r}\sum_{l=2}^{\infty}\sum_{m=0}^{l}\left(\frac{R}{r}\right)^l\left[\left(C_{l,m} - C_{l,m}^{el}\right)\cos m\lambda + S_{l,m}\sin m\lambda\right]P_{l,m}(\sin\varphi)\,, \tag{C5}$$

where $G = 6.674\times10^{-11}$m^{3}kg^{-1}s^{-2}, is the gravitational constant; $M = 5.9736\times10^{24}$ kg, is the mass of the Earth; r is the radial distance with $z = r - R$; $P_{l,m}(\sin\varphi)$ are the Legendre associated functions with (l, m) the degree and order of the harmonic expansion; ($C_{l,m}, C_{l,m}^{el}, S_{l,m}$) are the harmonic geopotential coefficients (Stokes parameters with $C_{l,m}^{el}$ belonging to the reference ellipsoid. From Eqs. (C1) and (C3) the potential of the true gravity is given by

$$V = T - g(\varphi)z\,. \qquad \text{(C6)}$$

From Eq.(C4) the true gravity is represented by

$$\mathbf{g}(\lambda,\varphi,z) = \nabla T + \left[\frac{\partial T}{\partial z} - g(\varphi)\right]\mathbf{k} \qquad \text{(C7)}$$

Appendix D. An Approximate 3D True Gravity Field for the Troposphere

According to Eq.(C5) (i.e., the spectral of the disturbing static gravity potential T), the ratio between $T(\lambda, \varphi, z)$ to $T(\lambda, \varphi, 0)$ through the troposphere can be roughly estimated by

$$\left|\frac{T(\lambda,\varphi,z)}{T(\lambda,\varphi,0)}\right| \approx \frac{R}{(R+z)} \approx 1, \qquad H \geq z \geq 0 \qquad \text{(D1)}$$

where H = 10.4 km, is the height of the troposphere. Since R is the radius of the Earth and more than 3 orders of magnitude larger than H. This leads to the first approximation that the disturbing gravity potential $T(\lambda, \varphi, z)$ does not change with z in the whole troposphere (approximation of thin layer for the troposphere)

$$T(\lambda,\varphi,z) \approx T(\lambda,\varphi,0), \qquad H \geq z \geq 0 \qquad \text{(D2)}$$

which makes

$$\nabla^2 T(\lambda,\varphi,z) \approx \nabla^2 T(\lambda,\varphi,0); \qquad \text{(D3)}$$

The potential of the true gravity satisfies the Laplace equation outside the Earth surface (Vaniček & Krakiwsky, 1986),

$$\nabla^2 V + \frac{\partial^2 V}{\partial z^2} = 0 \qquad \text{(D4)}$$

Substitution of (C6) into (D4) leads to the Laplace equation for the disturbing static gravity potential

$$\nabla^2 T + \frac{\partial^2 T}{\partial z^2} = 0 \qquad \text{(D5)}$$

Use of the second formula in (C4) gives

$$\nabla \bullet \mathbf{g}_h = -\frac{\partial^2 T}{\partial z^2} \approx -\frac{\partial^2 T}{\partial z^2}\Big|_{z=0} \qquad \text{(D6)}$$

where the approximation (D3) for the troposphere is used.

Acknowledgements

The author thanks Mr. Chenwu Fan's outstanding efforts on computational assistance, and the International Centre for Global Erath Models (ICGEM) for the second radial derivative of the disturbing static gravity potential ($\partial^2 T / \partial z^2$) data from the EIGEN-6C4 model, which is publicly available at the website: http://icgem.gfz-potsdam.de/home.

References

Chu, P.C. (2015). Ekman spiral in horizontally inhomogeneous ocean with varying eddy viscosity. *Pure and Applied Geophysics*, *172*, doi: 10.1007/s00024-015-1063-4.

Chu, P.C. (2021). Ocean dynamic equations with the real gravity. *Nature Scientific Reports*, *11*, Article Number 3235.

Ekman, V. W. (1905). On the influence of the earth's rotation on ocean-currents. *Arkiv för Matematik, Astronomi Och Fysik*, *2*, 1–52.

Gill, A.E. (1982). *Atmosphere-ocean dynamics*. *International geophysics series* (Vol 30), Academic Press, New York, 91-94.

Hackney, R.I., & Featherstone, W.E. (2003). Geodetic versus geophysical perspectives of the 'gravity anomaly'. *Geophysical Journal International*, *154*, 35-43.

Holton, J.R. (2004). An introduction to dynamic meteorology. Elsevier, Amsterdam, 131-136.

Kostelecký, J., Klokočnìk, J., Bucha, B., Bezděk, A., & Förste, C. (2015). Evaluation of the gravity model EIGEN-6C4 in comparison with EGM2008 by means of various functions of the gravity potential and by BNSS/levelling. *Geoinformatics FCE CTU*, *14 (1)*, http://doi.org//10.14311/gi.14.1.1.

National Geospatial-Intelligence Agency (1984). *Department of defense world geodetic system 1984 (WGS84).* Its definition and relationships with local geodetic systems. NIMA TR8350.2., 3rd Edition, Equation 4-1.

Pedlosky, J. (1987). *Geophysical fluid dynamics* (Second Edition), Springer, New York, 200-212.

Sandwell, D.T., & Smith, W.H.F. (1997). Marine gravity anomaly from Geosat and ERS 1 satellite altimetry. *Journal of Geophysical Research, 102*, 10,039-10,054

Sun, W.-Y., & Sun, O.M. (2020). Inertia and diurnal oscillations of Ekman layers in atmosphere and ocean. *Dynamics of Atmosphere and Oceans*, *90*, 101144.

Vaniček, P, & Krakiwsky, E. (1986). *Geodesy: the concepts*. Part 5 Earth gravity field, North-Holland, Amsterdam, 457-581.

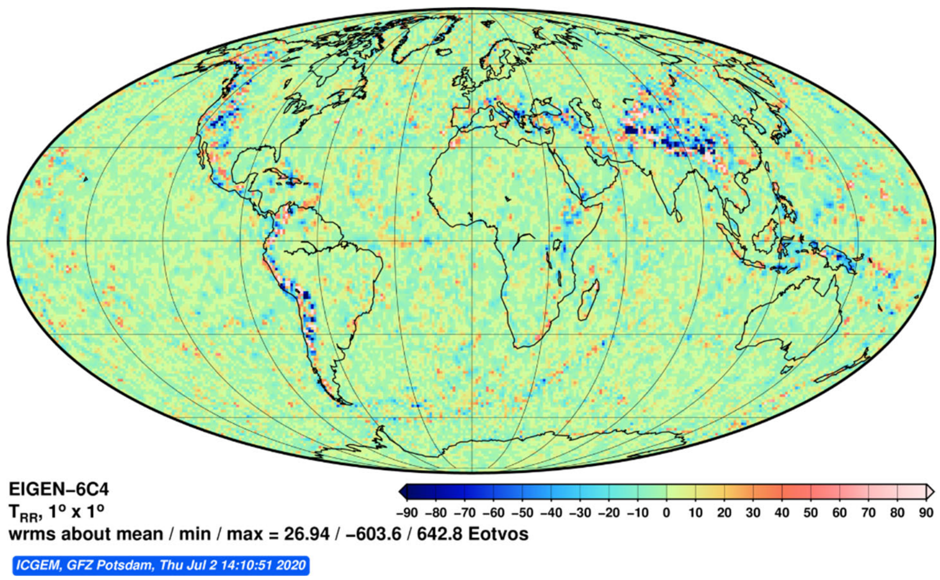

Figure 1. Global second radial derivative of the disturbing static gravity potential ($\partial^2 T / \partial z^2$) (unit: Eotvos) at z = 0 from the EIGEN-6C4 with 1°×1°, computed online at the website http://icgem.gfz-potsdam.de/home. Large positive (negative) values indicate evident upward (downward) Ekman pumping velocity due to the true gravity in the Northern Hemisphere, and opposite in the Southern Hemisphere.

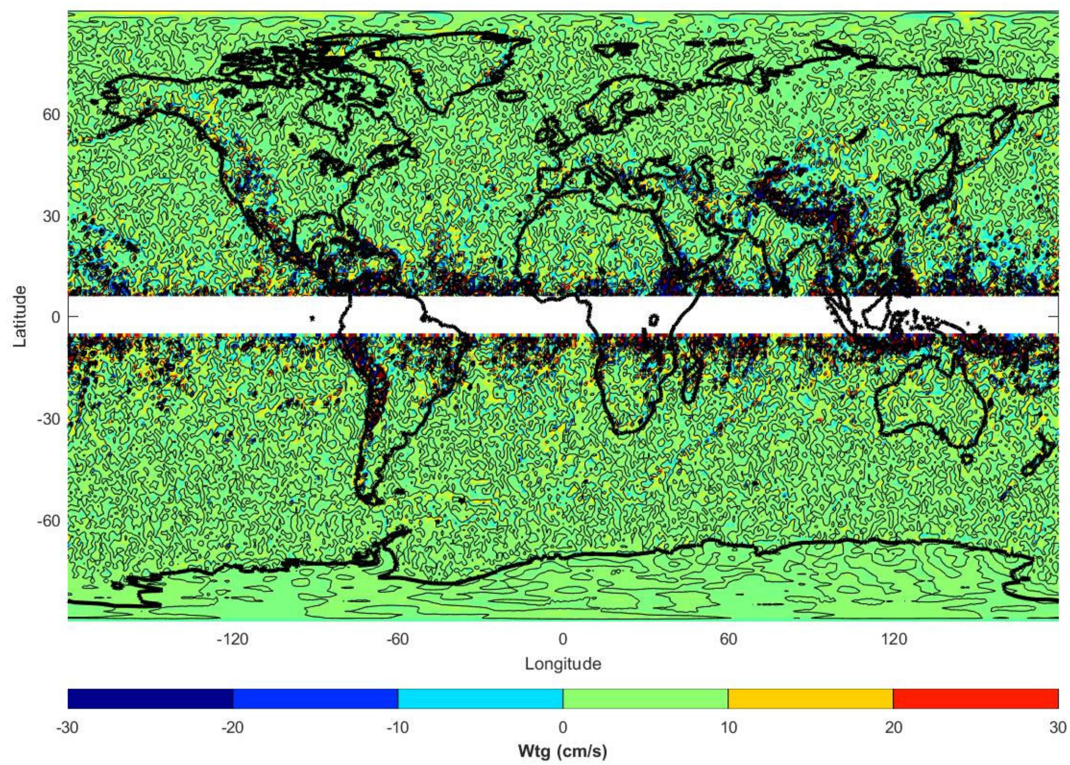

Figure 2. Ekman pumping velocity (cm s^{-1}) due to the use of the true gravity $w_{tg}(D_E)$ calculated with the EIGEN-6C4 $\partial^2 T / \partial z^2$ data.

(a)

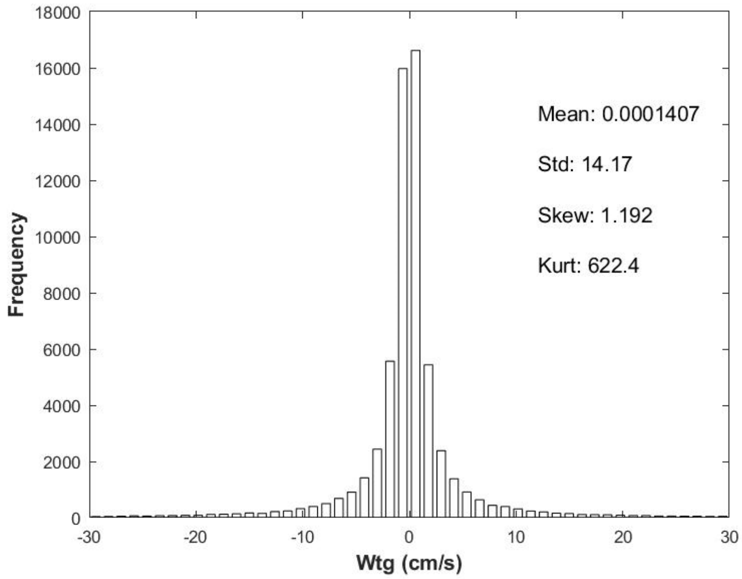

(b)

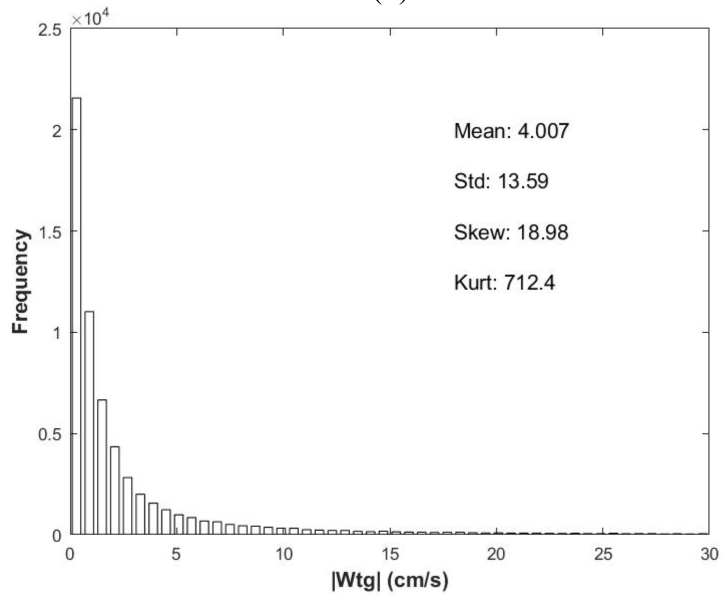

Figure 3. Histograms of global (a) $w_{tg}(D_E)$ and (b) $|w_{tg}(D_E)|$ (cm s^{-1}) with statistical parameters calculated using the EIGEN-6C4 $\partial^2 T / \partial z^2$ data.